An evaluation of preseason abundance forecasts for Sacramento River winter Chinook salmon

Michael O'Farrell[1]

Noble Hendrix[2]

Michael Mohr[1]

[1]Fisheries Ecology Division

Southwest Fisheries Science Center

National Marine Fisheries Service, NOAA

110 Shaffer Road

Santa Cruz, CA 95060

[2]QEDA Consulting, LLC

4007 Densmore Ave N

Seattle, WA 98103

October 3, 2016

1 Introduction

The Sacramento River winter Chinook salmon (SRWC) 2010 Biological Opinion (NMFS, 2010) for ocean fisheries concluded that fisheries are likely to jeopardize their continued existence owing to the lack of a management mechanism able to constrain or reduce fishery impacts when the SRWC population status is poor. As a result, the Reasonable and Prudent Alternative (RPA) specified that new fisheries management objectives and tools must be developed (NMFS, 2012). The RPA was first implemented in 2012, and resulted in a two-part consultation standard. The first component consisted of continuing the fishing season start and end date constraints and minimum size limits first implemented following the 2004 Biological Opinion (NMFS, 2004). The second component consisted of a control rule that limited the maximum allowable age-3 impact rate on SRWC south of Point Arena, California, based on the most recent 3-year geometric mean number of spawners. (Figure 1).

Use of the retrospective 3-year geometric mean number of spawners to set maximum allowable impact rates through the control rule was a consequence of limits in the available data. For many salmon stocks, age-2 (jack) return estimates are available prior to the Pacific Fishery Management Council (PFMC) preseason salmon management process, and these estimates are used to make preseason stock abundance forecasts. These jack returns can be a good indicator of year class strength, as they have survived the high and often variable mortality rates associated with downstream migration and early ocean residence. However, SRWC jack return estimates are not available in the winter/spring when abundance forecasts are needed for fishery planning. SRWC return to the river in winter, but delay spawning until the summer. Estimates of SRWC jack returns are first available in the fall, however, by this time, the portion of that cohort that did not mature but remained in the ocean has already been exposed to ocean salmon fisheries. Hence, jack return estimates cannot be used in a timely fashion for forecasting the abundance of the dominant age-3 cohort using the common sibling regression approach.

A control rule that relies only on past abundance or escapement to specify allowable exploitation rates is unable to respond to rapid changes in population status. For SRWC, recent indicators

strongly suggest a rapid decline in juvenile abundance coincident with the recent severe drought in California. In particular, fry abundance estimated at Red Bluff Diversion Dam (RBDD), located in the upper Sacramento River, was extremely low for the 2014 and 2015 broods. The 2014 brood encountered 2016 ocean fisheries as age-3 fish while the 2015 brood will encounter 2017 ocean fisheries as age-3 fish. In the absence of an abundance forecast that could incorporate this and other information on year class strength, the control rule cannot effectively serve its intended purpose of reducing exploitation rates as population status declines. The purpose of this report is to explore alternative abundance forecasting procedures for SRWC that integrate leading indicators of year class strength.

The general forecasting approaches considered here are based on an extension of an existing SRWC population dynamics model (Winship et al., 2011, 2014). The Winship et al. model was originally developed for obtaining parameter estimates for a management strategy evaluation (Winship et al., 2012, 2013), although its structure and parameterization lend itself to forecasting applications as well. The model is stochastic and structured by age, sex, and origin (natural and hatchery). It is fitted to data on natural-origin female spawners and fry abundance at RBDD. For natural-origin fish, the relationship between egg production and fry abundance is described by a Beverton-Holt model. The survival rate between the fry stage at RBDD and the end of the first year in the ocean, which includes both freshwater, estuarine, and ocean sources of mortality, is assumed to be density independent. External estimates of adult survival and maturation rates are then applied to complete the life cycle. To perform forecasts in practice, a model with a structure very similar to the Winship et al. model is fitted to the available data each year. A subset of the estimated parameters from the population dynamics model is then used to parameterize the forward projection forecast model. Notation used in this report (Table 1) follows that used in Winship et al. (2014).

The forecast metric is the SRWC age-3 escapement in the absence of fisheries, E_3^0. Confining the forecast to age-3 is appropriate for SRWC because there is strong evidence from coded-wire tag (CWT) recovery data that the age-2 and age-4 cohorts are rarely taken in ocean fisheries (O'Farrell et al., 2012). Age-2 fish are smaller than contemporary minimum size limits in ocean recreational

fisheries, which have ranged from 20 to 24 inches in total length, and thus are not retained. The average maturation rate of hatchery-origin age-3 fish for broods 1998–2010 has been estimated to be approximately 95 percent (O'Farrell, M.R., *unpublished data*), therefore only a small fraction of a SRWC cohort remains in the ocean and is exposed to fisheries as age-4 fish. Expressing SRWC abundance in terms of escapement absent fishing mortality allows for a more straightforward interpretation than, for example, ocean abundance prior to fishing. It is also consistent with the characterization of abundance for Sacramento River fall Chinook and Klamath River fall Chinook when applying their respective control rules during the PFMC fishery planning process.

In this report we describe the proposed forecasting approach and modifications made to the Winship et al. population dynamics model. We identify three alternative forecasting models based on different levels of model complexity and the availability of natural-origin juvenile abundance estimates. The performance of the forecast models is then evaluated using one year ahead cross validation. We end with a recommendation of a preferred forecast model.

2 Forecast model specification

Forecasts of SRWC age-3 escapement in the absence of fishing in year t is the sum of sex- ($s \in \{m = \text{male}, f = \text{female}\}$) and origin- ($o \in \{n = \text{natural}, h = \text{hatchery}\}$) specific forecasts of $E^0_{t,3}$,

$$ {}^{w}\hat{E}^0_{t,3} = \sum_s \sum_o {}^{w}\hat{E}^0_{t,3,s,o}, \tag{1} $$

where

$$ {}^{w}\hat{E}^0_{t,3,s,o} = \begin{cases} 0.5 \times {}^{w}J_{t-3} \times {}^{w}j_{t-3} \times (1-\tau_{2,s}) \times (1-\eta_3) \times \tau_{3,s}, & \text{if } o = n \\ 0.5 \times P_{t-3} \times \kappa \times {}^{w}j_{t-3} \times (1-\tau_{2,s}) \times (1-\eta_3) \times \tau_{3,s}, & \text{if } o = h. \end{cases} \tag{2} $$

Sex-specific, natural-origin forecasts in year t begin with the estimated number of fry at RBDD (J) in year $t-3$ and the assumption of a 0.5 sex ratio at this stage. Fry production is then multiplied by the juvenile survival rate j to account for survival of fry to the end of age-2 in the ocean.

Accounting for sex- and age-specific maturation rates (τ) and the ocean age-3 natural mortality rate η_3 results in the forecast escapement absent fishing. For hatchery-origin fish, the forecast begins with the number of pre-smolts released from Livingston Stone National Fish Hatchery (P), along with an assumed sex ratio of 0.5. Survival from the pre-smolt stage to the end of age-2 in the ocean is the product of the natural-origin juvenile survival rate and the hatchery:natural juvenile survival rate ratio κ. The maturation and natural mortality rates used for natural-origin fish are also used for hatchery-origin fish.

Equation 2 presents the forecast model as a product of scalars, however the quantities J and j are modeled as distributional quantities, with the 'w' prescript denoting a particular random draw (w) from the bivariate J, j distribution and the corresponding $\hat{E}^0$ value. The nature of these distributions is described in more detail below and in Sections 3 and 4. The variable P is specified annually, but is assumed to be measured without error. Variables τ and η are singular values that do not vary over time. Hence, the resulting forecast of $\hat{E}^0_{t,3}$ is a distribution where the precision of the forecast is a function of the precision of the distributions describing J and j.

Estimates of J, and their sampling error, are routinely made by the United States Fish and Wildlife Service (USFWS) based on rotary screw trapping at RBDD. For the forecasts described herein, J is the fry-equivalent Juvenile Production Index (JPI) as described in Poytress et al. (2014). The fry-equivalent JPI consists of estimated natural-origin SRWC-sized juveniles passing RBDD, standardized to the fry stage[1]. The standardization consists of dividing the estimated number of pre-smolt and smolt-sized SRWC by 0.59 to account for the estimated survival between the fry and pre-smolt/smolt stage and adding this to the estimated number of SRWC fry. Use of the fry-equivalent JPI allows for a measure of SRWC juvenile production from the upper Sacramento River that is standardized by the fry developmental stage, which facilitates comparison of production across years and, ultimately, the fitting of the egg-to-fry stock recruitment model.

The number of pre-smolts P released from Livingston Stone National fish hatchery is enu-

[1]Juvenile SRWC trapped at RBDD are very unlikely to be of hatchery-origin because nearly 100% of hatchery production is marked with an adipose fin clip and tagged with a CWT. Additionally, natural-origin juveniles generally pass RBDD before the end of December while hatchery production is nearly always released in February.

merated annually and these data are publicly available from the Regional Mark Processing Center (`http://www.rmpc.org`). Because hatchery releases are censused rather than estimated, we assume that P is measured without error and is treated as a known value.

The distribution of the juvenile survival rate for natural-origin fish j was estimated within the Winship et al. (2011, 2014) model framework. Estimates of the hatchery:natural juvenile survival rate ratio κ were derived by applying the ratio of means estimator to the hatchery-origin and natural-origin juvenile survival rate time series (Winship et al., 2014), where the hatchery-origin juvenile survival rates were estimated using cohort reconstruction methods (O'Farrell et al., 2012, and O'Farrell, M.R. *unpublished data*), and the natural-origin juvenile survival rates were estimated from the Winship et al. (2011, 2014) model.

Age- and sex-specific maturation probabilities τ were estimated from data on the age composition of hatchery-origin spawners (see Winship et al., 2014, Supplement B). For the forecasts presented here, we used the estimated values of $\tau_{a,s}$ reported in Winship et al. (2014).

Age-3 ocean natural mortality rates η_3 were assumed to be constant at 0.20. This value is consistent with the natural mortality rate used in the SRWC cohort reconstruction (O'Farrell et al., 2012) and other salmon assessment models (e.g., Mohr, 2006).

Looking forward, in some years it may not be possible to obtain empirical estimates of the fry-equivalent JPI. This may occur due to funding lapses (as occurred in 2000 and 2001), environmental conditions, Shasta Reservoir flood releases, or other unanticipated complications. In the case where an empirical estimate of the fry-equivalent JPI is unavailable, we need a means to forecast natural-origin SRWC abundance using a model-based prediction of J. In the following Sections, we describe the forecast approach that will be used when an empirical estimate of the fry-equivalent JPI is available, and the forecast approach that will be used in the absence of such an estimate (Figure 2).

3 Population dynamics model

A population dynamics model was fitted to updated natural-origin female spawner and natural-origin fry data for use in generating select inputs into the forecast model (Equations 1 to 2). Because the population dynamics model is a variant of the Winship et al. (2014) model, we do not specify the entire model structure here but rather refer to the paper in which the model is fully documented and describe only the modifications made to that model. The modifications include (1) the addition of an environmental covariate to the egg-to-fry relationship, and (2) the addition of a biological covariate to the juvenile survival rate.

3.1 Egg-to-fry relationship modifications

The transition from egg to fry is described by the Beverton-Holt model

$$J_t = \frac{\theta_1 g_t F_t}{1 + \theta_2 g_t F_t}, \tag{3}$$

where F_t is the year t number of natural-area female spawners and g_t is the year t number of eggs per female. This parameterization of the Beverton-Holt model follows that used in Winship et al. (2014), with the exception that year-specific fecundity is used here while a fixed number of eggs per female value was used in Winship et al. (2014).

The egg-to-fry model was further modified by the addition of an environmental covariate to better account for observed annual variation. The temperature-based covariate (X_t) is the number of degree days above a critical temperature (T_{crit}) threshold, evaluated over the May 15–October 31 temperature compliance period for the upper Sacramento River,

$$X_t = \sum_{d=\text{May 15}}^{d=\text{Oct 31}} \max(\overline{T}_{t,d} - T_{crit}, 0), \tag{4}$$

where $\overline{T}_{t,d}$ is the average temperature for day d in year t. Daily means were calculated from hourly temperature data obtained from a gauge located in the upper Sacramento River near Bon-

nyview Bridge and upstream of the confluence of Clear Creek (S. John, Fisheries Ecology Division/SWFSC/NMFS, *personal communication*, based on data obtained at `http://cdec.water.ca.gov/cgi-progs/stationInfo?station_id=CCR`). The gauge location is near the downstream end of SRWC spawning activity in recent years. We assumed a T_{crit} value of 12°C, based on the results of a biophysical model described in Martin et al. (2016).

The temperature covariate was included in the egg to fry relationship by specifying the maximum egg to fry survival rate in the absence of density dependence (θ_1) as a function of X_t,

$$\text{logit}(\theta_{1,t}) = \gamma_0 + \gamma_1 X_t, \tag{5}$$

where $\text{logit}(\theta_1) = \log[\theta_1/(1-\theta_1)]$. This formulation results in annual variation of the density-independent egg-to-fry survival parameter.

3.2 Juvenile survival rate modification

In the Winship et al. (2014) model, the juvenile survival rate was estimated as a year-specific random effect drawn from a beta distribution. However, there was evidence that estimates of the juvenile survival rate were positively correlated with the empirical egg-to-fry survival rate estimates. Therefore, we considered an alternative parameterization in which the juvenile survival rate was modeled as a function of the egg-to-fry survival rate.

To evaluate the potential for the empirical egg-to-fry survival rate (Table 3) to predict the juvenile survival rate j, we constructed a model with the empirical egg-to-fry survival rate estimate as a covariate for the annual estimation of j. The empirical egg-to-fry survival rate estimate equaled the juvenile fry equivalents at RBDD divided by the number of natural-origin eggs in a given year. The value of j was modeled as

$$\text{logit}(j_t) = \delta_0 + \delta_1 Z_t + \varepsilon_t, \quad \varepsilon_t \sim N(0, \sigma^2 = 1/\omega) \tag{6}$$

where Z_t was the logit of the empirical egg-to-fry survival rate estimate and ω is the precision

of the annual random effects, ε_t. Values of δ_1 near zero indicates the model has little predictive ability.

3.3 Estimation and Priors

We fit the models using JAGS (Just Another Gibbs Sampler; Plummer, 2016) in the same Bayesian framework as Winship et al. (2014). For the Bayesian estimation, we developed prior distributions for all model parameters with the goal of specifying vague conjugate priors to facilitate Gibbs sampling (Table 4). For the parameters of the logistic regressions, the prior density must be concentrated in the region where the logistic function is most sensitive; therefore, coefficients of the logistic regressions (γ and δ) were given normal priors with a variance of 4. Similarly the precision of the random effects ω must also be given a prior that is appropriate for the logistic regression, thus it was assigned a gamma G(3,3) prior (Table 5). See King et al. (2009) for further discussion of prior distributions for logistic regression models.

4 Forecast scenarios

The first forecast scenario, referred to as *Base*, assumed that an empirical estimate of the JPI was available. Here, J is a lognormally distributed random variable, where $J_t \sim \text{LN}(\log(\text{JPI}_t), \sigma_t^2)$ and σ_t^2 is the annual measurement error variance derived from the CV(J_t) estimates in Table 2. For lognormal distributions, $\sigma^2 = \log(\text{CV}^2 + 1)$. The egg-to-fry relationship included the temperature covariate X as described in Section 3.1. Values of the juvenile survival rate j were randomly sampled from a beta distribution fitted to estimates of j_t.

The second forecast scenario, referred to as *ETF*, is the same as the *Base* scenario except that the juvenile survival rate is modeled as a function of Z_t, as described in Section 3.2, instead of being randomly sampled from a beta distribution.

The third forecast scenario, referred to as *no JPI*, assumed the same population dynamics model as *Base*, but instead of using an empirical estimate of the JPI, a model-based value was used instead. Values of J_t were therefore derived from the egg-to-fry relationship as described in

Section 3.1. Values of the juvenile survival rate j were randomly sampled from a beta distribution fitted to estimates of j_t. We did not consider a model where j was estimated using the Z_t covariate for the *no JPI* scenario, because if an empirical estimate of the JPI is unavailable, an empirical estimate of the egg-to-fry survival rate is also unavailable.

5 Cross validation

To evaluate the alternative forecast scenarios, we employed a cross validation approach that mimics the relevant steps in the forecasting process. In particular, the cross validation uses data through a given calendar year t and makes a forecast of $\hat{E}^0_{t,3}$ given J_{t-3} and the other quantities in equation 2. The cross validation steps are as follows for each calendar year $t = 2012$ to $t = 2015$ (brood years 2009 to 2012, respectively), allowing for 4 years of one-year ahead forecasts.

1. Fit estimation model to data through year $t-2$ to obtain relevant parameter estimates.
2. Use the distribution of J_{t-3} (specific to each forecast scenario) to forecast $\hat{E}^0_{t,3}$.
   (a) Construct the distribution of J_{t-3} using the estimated JPI and CV(J_{t-3}), or when the JPI is unavailable, by obtaining the posterior distribution of J_{t-3}.
   (b) Calculate $\hat{E}^0_{t,3,s,o=n}$ as a function of (J_{t-3}, j_{t-3}, η, τ) using equation 2.
   (c) Calculate $\hat{E}^0_{t,3,s,o=h}$ as a function of (P_{t-3}, $j_{t-3}, \kappa, \eta, \tau$) using equation 2.
   (d) Calculate $\hat{E}^0_{t,3}$ using equation 1.
3. Compare forecasts of $\hat{E}^0_{t,3}$ to $E^0_{t,3}$. Postseason estimates of $E^0_{t,3}$ were derived from adult SRWC escapement estimates obtained from Table B-3 in PFMC (2016), the average proportion of adult escapement that was age-3 ($\overline{p}_3$) estimated from CWT data (M. O'Farrell, *unpublished data*), and the age-3 fishery impact rate (i_3), estimated from cohort reconstructions (M. O'Farrell, *unpublished data*):

$$E^0_{t,3} = \frac{E_{t,a\geq 3} \times \overline{p}_3}{(1 - i_{t-1,3})}. \tag{7}$$

Forecasts were compared to postseason estimates using two pointwise prediction error metrics and one distribution-based prediction error metric:

(a) Mean error (ME)

$$\mathrm{ME} = \frac{\sum_t (E^0_{t,3} - \hat{E}^0_{t,3})}{n}, \tag{8}$$

(b) Root mean square error (RMSE)

$$\mathrm{RMSE} = \sqrt{\frac{\sum_t (E^0_{t,3} - \hat{E}^0_{t,3})^2}{n}}, \tag{9}$$

(c) Log pointwise predictive density (LPPD)

$$\mathrm{LPPD} = \frac{1}{n} \sum_t \log \left(\frac{\sum_w \mathrm{P}(E^0_{t,3} | {}^w\hat{E}^0_{t,3})}{W} \right) \tag{10}$$

where $n = 4$ is the number of one-year ahead forecasts, w is a sample from the distribution of $\hat{E}^0_{t,3}$, and P is the sampling probability distribution, which is a lognormal probability density function specified with bias corrected mean and variance using the annual sampling coefficient of variation, $\mathrm{CV}(F_t)$.

Values of ME, RMSE, and LPPD are expressed as averages over the four one-year ahead forecasts.

6 Results

We describe the results of fitting the *Base* and *ETF* formulations of the population dynamics model to the entire data series (Table 2). We then assess forecast performance by examining summary statistics derived from the one-year ahead cross validation procedure.

6.1 Base model

The fitted model closely tracked the number of female natural-origin spawners owing to the low levels of measurement error assumed for these estimates (Figure 3). Estimates of natural-origin fry were assumed to be less precise than the estimated numbers of natural-origin spawners and therefore the fits did not track this time series as tightly (Figure 3).

Figure 4 displays the egg-to-fry relationship with the θ_1 parameter specified at the mean value of the temperature covariate X_t. The relationship is not able to adequately explain some of the annual variation in the data. When year-specific fits of the Beverton-Holt model informed by X_t are examined, the annual variation in the number of fry are much better described (Figure 5). In many years, the year-specific fits approximate the data better than the model evaluated at the mean level of X_t (represented by dashed lines). In particular, the broods with very low egg-to-fry survival (brood years 2014 and 2015) are well described when the year-specific temperature covariate is included.

Figure 6 displays how the temperature covariate affects the maximum egg-to-fry survival rate. The relationship demonstrates the predicted result that more exposure to elevated water temperatures (above T_{crit}) is associated with lower egg-to-fry survival (Martin et al., 2016).

Estimates of the juvenile survival rate suggest that survival is relatively low in most years, but punctuated by years with relatively high survival (Figure 7). This result is consistent with that reported in Winship et al. (2014) and for other salmon stocks (see Winship et al., 2011, Appendix D).

Hatchery-origin juvenile survival rates, estimated from cohort reconstructions (O'Farrell et al., 2012, and O'Farrell, M.R. *unpublished data*) were positively correlated with juvenile survival rates estimated for natural-origin fish (Figure 8). This relationship was consistent with the results in Winship et al. (2014). The slope of the zero-intercept linear model, estimated using the ratio-of-means estimator (κ), was 1.9. The estimated value was similar to to the value of $\kappa = 2.3$ reported in Winship et al. (2014).

6.2 ETF model

The *ETF* model fit the escapement and juvenile abundance index data similarly to the *Base* model. The annual variation in escapement data was tracked well by the model, whereas fits to the juvenile data were less accurate. Because the fits to these time series in the *Base* and *ETF* models were so visually similar, a figure displaying the *ETF* model fits is not displayed.

The parameter values describing the relationship between the temperature covariate X_t and the egg-to-fry survival rate were also similar in both the *Base* model (Table 4), and the *ETF* model (Table 5). As a result the, stock recruitment relationship under the *ETF* model was visually very similar to the relationship under the *Base* model, and thus it is not displayed here.

The juvenile survival rate j was positively related to the empirical egg to fry survival rate (Figure 9). Uncertainty in the relationship was attributable to parameter uncertainty and the annual random effects. The relationship between the juvenile survival rate j and the empirical egg-to-fry survival rate Z was positive with the δ_1 parameter value having a positive median value and 95% credible interval values greater than 0 (Table 5). The uncertainty in the relationship due to parameter uncertainty (dark gray region in Figure 9) also captured the effect of the range of Z values; the smallest intervals were located near the center of the Z values and expanded at higher values of Z due to fewer observations.

In addition to the positive relationship between j and Z, there was additional variability captured in the annual random effects (ε_t). This additional variability is displayed in the light gray areas in Figure 9. Not all years contributed equally to the estimated precision (ω) of the random effects, however. The 1999 juvenile survival rate was the highest estimated rate in the time series, yet the empirical egg to fry survival rate was at an intermediate value in this year (Figure 9). As a result of this relationship, the estimated precision of the random effects was likely heavily influenced by the 1999 data values.

6.3 Cross validation

Forecasted $\hat{E}_3^0$ under the *Base* model and the *no JPI* model were similar, whereas forecasted $\hat{E}_3^0$ under the *ETF* model tended to be less precise (Figure 10). Metrics that compared point estimates of forecasting accuracy indicated that the *Base* model was the most accurate of the three models, and furthermore, the mode was a more accurate point estimate than the median (Tables 6 and 7). The LPPD metric, which takes into account the posterior distribution of $\hat{E}_{t,3}^0$ and the sampling distribution of $E_{t,3}^0$, also indicated that the *Base* scenario performed better than *ETF* scenario.

Plots of the forecasted distributions indicated general characteristics of each model (Figure 10). In general, the *Base* model provided the most precise forecasts (with the exception of 2012), whereas the *ETF* model provided the least precise forecasts, and the *no JPI* model was intermediate. Differences in the precision between *Base* and *no JPI* forecasts were due to differing estimates of the juvenile abundance J_t. For forecast year 2012 (brood year 2009) J_t was approximately 5 million fry, and accounting for the sampling variance under the *Base* model led to a more diffuse estimate of J_t than using the model-based estimate under *no JPI*. In the other years, the distribution of J_t under the *no JPI* model was more diffuse.

The precision of forecasts under *ETF* was affected by the magnitude of the random effects variance and the parameter uncertainty in the regression coefficients for j_t in Equation 6. The precision of the *ETF* forecasts increased over the 4 years as additional data were used to improve the estimates of the regression coefficients. Future one-year ahead forecasts using the *ETF* model may be more precise than those presented in Figure 10. For example, to forecast 2015, the *ETF* model was fit to data through 2013, thus an additional 2 years of data were used to obtain the estimates in Table 5.

The accuracy of forecasts under the *Base* and *no JPI* models was affected by the mode of the beta distribution for j, relative to the true, but unobserved, juvenile survival rate. While we do not know the true underlying juvenile survival rate exactly, we can compute an approximation of this value post-hoc as $\tilde{j}_t = E_{t,3,o=n}^0 / J_{t-3}$, where $E_{t,3,o=n}^0 = E_{3,t}^0 \times (1 - h_t)$. The direction of the annual value of this post-hoc estimate relative to its median provides an indication of the relative

survival rate after RBDD (Table 8). Because the *Base* and *no JPI* models do not incorporate annual variability in juvenile survival, the accuracy of the forecast depends on whether the true juvenile survival rate is close to the median. That is, accurate forecasts under these models will occur when the true j is near the median of past estimates. Deviations between $\hat{E}^0_{t,3}$ and $E^0_{t,3}$ will occur when the true j varies from the median. The direction of the error (under predicting versus over predicting) will be in the opposite direction of variation in the annual post-hoc estimate of j. For example, in 2012 the *Base* model over-predicted the $E^0_{t=2012,3}$ because the post-hoc $\tilde{j}$ was below the median. In contrast, in 2013, 2014, and 2015, the post-hoc estimates of $\tilde{j}$ were all above the median, and the *Base* model under predicted the $E^0_{t,3}$ in those years (Figure 10).

The accuracy of the forecasts under the *ETF* model is related to the value of the Z_t covariate and the true, but unobserved, juvenile survival rate. We can obtain insight into the potential value of this approach in the future by simple comparison of $\tilde{j}$ to Z. There does appear to be congruence, at least in the relative direction, of the post-hoc $\tilde{j}$ and the value of Z that is appropriate for that year (Table 8) suggesting that there may be utility to using the Z values for forecasting purposes.

7 Discussion

In this report, a set of candidate SRWC abundance forecast models are described. Two of these models (*Base* and *ETF*) require estimates of the fry-equivalent JPI and it's sampling error, while a third model (*no JPI*) is able to forecast abundance in the absence of these estimated quantities. Forecast performance was assessed by performing one-year ahead cross validation in a manner that mimics how the abundance forecasts would be made in practice during the annual PFMC salmon fishery planning process. Summary performance metrics (ME, RMSE, LPPD) and visual inspection of forecast distributions versus postseason-estimated values were used to assess overall forecast model performance.

With regard to the case when estimates of the JPI and it's sampling error are available, the *Base* model outperformed the *ETF* model. Values of ME, RMSE, and LPPD for the *Base* model indicated better forecast performance relative to the *no JPI* model. Furthermore, visual inspection

of the forecast distributions versus postseason estimates of $E^0_{t,3}$ indicated that the *Base* model produced forecasts with much greater precision than the *ETF* model. For the *Base* model, the mode of the $\hat{E}^0_{t,3}$ distribution resulted in slightly less biased and more accurate forecasts relative to the median. Forecast performance of the *no JPI* model was similar to the *Base* model, suggesting that the *no JPI* model could be a viable alternative if estimates of the JPI and it's sampling error are not available in a given year.

The short time series of data and the number of estimated parameters for the three models considered severely limited the number of years for which we could perform one-year ahead cross validation. Attempts to perform one-year ahead forecasts for a greater number of years resulted in poor estimation properties and thus we limited our forecast versus postseason-estimated comparisons of $E^0_{t,3}$ to the final four years of data. Caution in over-interpreting the cross validation results is therefore warranted.

Despite having relatively poor forecast performance as assessed through the cross validation procedure, there does appear to be some information content gained from using egg-to-fry survival rates to inform forecasts of $E^0_{t,3}$. The precision of the $\hat{E}^0_{t,3}$ distributions under the *ETF* model increased with the addition of data, suggesting that as the data series matures the forecast performance could improve. There may be value in continuing to monitor the performance of the *ETF* model relative to the *Base* model as more data become available. Monitoring the forecast performance of the *ETF* model in the coming years could be potentially informative. Brood years 2014 and 2015 (ocean fishery forecast years 2016 and 2017) have the two lowest egg-to-fry survival rates on record (Table 3). If the positive correlation between Z and j holds, then the *Base* model could tend to over forecast $E^0_{t,3}$. However, it is uncertain whether the *ETF* model would make more accurate forecasts than the *Base* model for these years because j would be predicted using values of Z well outside the previously observed range of egg-to-fry survival rates.

8 Conclusions

Based on the results presented herein, we recommend using the *Base* model to forecast $E^0_{t,3}$ upon adoption of a new ocean fishery management framework for SRWC. Furthermore, we recommend using the mode of the $\hat{E}^0_{t,3}$ distribution as the measure of SRWC abundance used to set maximum allowable age-3 impact rates via a control rule. Performance of the *ETF* model will continue to be monitored with the accumulation of new data.

9 Acknowledgments

We would like to thank the members of the Ad Hoc Sacramento River Winter Chinook Workgroup for their assistance in the formulation of a SRWC abundance forecast. Contributing members of the Workgroup include Peter Dygert, Eli Holmes, Jeromy Jording, Brett Kormos, Jason Roberts, and Jim Smith. Thanks also goes to Mike Burner for facilitating the Workgroup. We would also like to thank Ben Martin, Eric Danner, and Sara John for sharing their expertise on the effects of water temperature on egg survival.

Table 1. Model notation.

Symbol	Definition
B	The number of natural-origin females removed from the river for broodstock
E^0	Escapement in the absence of fisheries
F	The number of natural-origin female spawers
h	The proportion of female spawners that were of hatchery origin
J	Fry abundance at Red Bluff Diversion Dam (fry-equivalent JPI)
j	Juvenile survival rate (fry to the end of age-2 in the ocean)
P	The number of pre-smolts released by the hatchery
T	Temperature measured at the Clear Creek gauge
T_{crit}	Critical temperature
$\overline{p}_3$	Mean proportion of adult ($a \geq 3$) escapement that is age-3
τ	Maturation rate
η	Natural mortality rate
κ	Ratio of hatchery-origin to natural-origin juvenile survival rates
θ_1	Maximum egg-to-fry survival rate in the absence of density dependence
θ_2	Strength of density dependence
γ	Coefficients in the equation defining maximum egg-to-fry survival as a function of critical temperature
δ	Coefficients in the equation defining juvenile survival rate j as a function of empirical egg-to-fry survival
ε	Annual random effects in the equation defining juvenile survival rate j as a function of empirical egg-to-fry survival
ω	Precision of random effects in the equation defining the juvenile survival rate
X	Temperature covariate for the egg-to-fry relationship
Z	Empirical egg-to-fry covariate for the estimation of juvenile survival
z	Adult survival rates
o	Index denoting origin $o \in$ {n = natural, h = hatchery}
s	Index denoting sex $s \in$ {m = male, f = female}
a	Index denoting age
t	Index denoting year
d	Index denoting day
w	Index denoting a sample from a distribution

Table 2. Data, parameters, and variables treated as known values.

Year	J_t	CV(J_t)	P_t	F_t	CV(F_t)	g_t	B_t	h_t	$z_{3,t}$	$z_{4,t}$
1996	469,183	0.38				4,926				
1997	2,205,163	0.31				4,926				
1998	5,000,416	0.16	153,908			3,372			0.63	
1999	1,366,161	0.19	30,840			4,256			0.63	0.48
2000			166,207	3,494	0.03	4,911	44	0.002	0.60	0.48
2001			252,278	5,014	0.03	4,737	45	0.052	0.58	0.69
2002	7,635,469	0.39	232,723	5,408	0.03	4,820	47	0.053	0.61	0.19
2003	5,781,519	0.24	218,617	4,972	0.01	4,854	48	0.047	0.71	0.35
2004	3,677,989	0.26	168,261	3,049	0.03	5,515	36	0.074	0.58	0.25
2005	8,943,194	0.28	173,344	7,203	0.01	5,473	52	0.204	0.65	0.47
2006	7,298,838	0.26	196,288	7,575	0.02	5,484	51	0.145	0.67	0.60
2007	1,637,804	0.21	71,883	1,442	0.05	5,112	21	0.070	0.65	0.80
2008	1,371,739	0.23	146,211	1,365	0.04	5,519	51	0.066	0.80	0.80
2009	4,972,954	0.27	198,582	2,366	0.07	5,351	57	0.131	0.80	0.80
2010	1,572,628	0.23	123,859	692	0.06	5,161	28	0.160	0.67	0.59
2011	996,621	0.2	194,264	426	0.06	4,831	49	0.132	0.55	0.00
2012	1,789,259	0.19	181,857	880	0.06	4,516	48	0.412	0.69	0.46
2013	2,481,324	0.23	193,155	3,400	0.06	4,596	60	0.076	0.63	0.63
2014	523,839	0.26	609,311	1,399	0.06	5,242	72	0.198	0.63	0.48
2015	440,951	0.21		1,592	0.06	4,819	78	0.228		

Table 3. Empirical egg-to-fry survival rate estimates, and their sources, used as a covariate to estimate the juvenile survival rate.

Brood year	Value	Source
1996	0.21	Poytress (2016)
1997	0.40	Poytress (2016)
1998	0.27	Poytress (2016)
1999	0.22	Poytress (2016)
2000	0.26	Base model estimate
2001	0.21	Base model estimate
2002	0.30	Empirical estimate computed from data in Table 2
2003	0.24	Empirical estimate computed from data in Table 2
2004	0.22	Empirical estimate computed from data in Table 2
2005	0.23	Empirical estimate computed from data in Table 2
2006	0.18	Empirical estimate computed from data in Table 2
2007	0.23	Empirical estimate computed from data in Table 2
2008	0.19	Empirical estimate computed from data in Table 2
2009	0.40	Empirical estimate computed from data in Table 2
2010	0.46	Empirical estimate computed from data in Table 2
2011	0.55	Empirical estimate computed from data in Table 2
2012	0.48	Empirical estimate computed from data in Table 2
2013	0.16	Empirical estimate computed from data in Table 2
2014	0.08	Empirical estimate computed from data in Table 2
2015	0.06	Empirical estimate computed from data in Table 2

Table 4. Prior and posterior distributions for the *Base* model. Prior distributions are denoted as follows: U(a, b) is the uniform distribution over the (a, b) interval, N(a, b) is the normal distribution with mean a and variance b, B(a, b) is the beta distribution with shape parameters a and b, and G(a, b) is the gamma distribution with shape parameter a and scale parameter b. A G(1e-3, 1e-3) prior was assigned to the precision of recruitment stochasticity rather than specifying a prior directly on CV_J.

			Posterior			
Parameter	Description	Prior	Mean	Median	0.025	0.975
J_{96}	number of fry	U(1e5, 1e9)	6.3e+05	5.9e+05	2.8e+05	1.2e+06
J_{97}		U(1e5, 1e9)	2.8e+06	2.7e+06	1.5e+06	4.6e+06
J_{98}		U(1e5, 1e9)	5.2e+06	5.2e+06	3.9e+06	7.0e+06
J_{99}		U(1e5, 1e9)	1.7e+06	1.7e+06	1.2e+06	2.4e+06
γ_0	θ_1 model parameter	N(0,4)	-1.9e-01	-2.6e-01	-7.9e-01	8.4e-01
γ_1	θ_1 model parameter	N(0,4)	-6.9e-03	-7.2e-03	-1.0e-02	-5.3e-03
θ_2	strength of density dependence	U(0, 1)	3.7e-08	3.3e-08	9.8e-09	9.2e-08
CV_J	CV of recruitment stochasticity	see caption	1.5e-01	1.3e-01	3.3e-02	3.8e-01
ϕ_1	mean fry survival probability	U(0, 0.5)	3.6e-03	3.5e-03	2.4e-03	5.5e-03
ϕ_2	variability in fry survival probability	U(0, $\sqrt{\phi_1}$)	4.8e-02	4.7e-02	3.3e-02	6.7e-02
j_{96}	fry survival probability	B(ϕ_1, ϕ_2)	3.5e-03	2.9e-03	2.0e-04	1.1e-02
j_{97}		B(ϕ_1, ϕ_2)	4.6e-03	4.4e-03	2.5e-03	7.7e-03
j_{98}		B(ϕ_1, ϕ_2)	3.4e-03	3.4e-03	2.4e-03	4.5e-03
j_{99}		B(ϕ_1, ϕ_2)	1.1e-02	1.1e-02	8.0e-03	1.6e-02
j_{00}		B(ϕ_1, ϕ_2)	3.8e-03	3.8e-03	2.5e-03	5.5e-03
j_{01}		B(ϕ_1, ϕ_2)	1.9e-03	1.8e-03	1.3e-03	2.9e-03
j_{02}		B(ϕ_1, ϕ_2)	4.1e-03	4.1e-03	2.6e-03	5.6e-03
j_{03}		B(ϕ_1, ϕ_2)	4.2e-03	4.2e-03	3.1e-03	5.6e-03
j_{04}		B(ϕ_1, ϕ_2)	1.2e-03	1.1e-03	8.3e-04	1.6e-03
j_{05}		B(ϕ_1, ϕ_2)	6.5e-04	6.4e-04	4.4e-04	9.0e-04
j_{06}		B(ϕ_1, ϕ_2)	8.4e-04	8.2e-04	5.5e-04	1.2e-03
j_{07}		B(ϕ_1, ϕ_2)	8.8e-04	8.6e-04	6.3e-04	1.2e-03
j_{08}		B(ϕ_1, ϕ_2)	1.2e-03	1.2e-03	8.0e-04	1.5e-03
j_{09}		B(ϕ_1, ϕ_2)	1.2e-03	1.2e-03	7.5e-04	1.6e-03
j_{10}		B(ϕ_1, ϕ_2)	6.3e-03	6.3e-03	4.6e-03	8.4e-03
j_{11}		B(ϕ_1, ϕ_2)	4.7e-03	4.7e-03	3.4e-03	6.2e-03
j_{12}		B(ϕ_1, ϕ_2)	2.4e-03	2.4e-03	1.8e-03	3.3e-03
j_{13}		B(ϕ_1, ϕ_2)	3.5e-03	2.7e-03	2.4e-04	1.1e-02

Table 5. Prior and posterior distributions for the *ETF* model. Prior distributions are denoted as follows: U(a, b) is the uniform distribution over the (a, b) interval, N(a, b) is the normal distribution with mean a and variance b, B(a, b) is the beta distribution with shape parameters a and b, and G(a, b) is the gamma distribution with shape parameter a and scale parameter b. A G(1e-3, 1e-3) prior was assigned to the precision of recruitment stochasticity rather than specifying a prior directly on CV_J. The juvenile survival rates j_t were computed from the logistic regression coefficients and thus do not have explicit priors.

			Posterior			
Parameter	Description	Prior	Mean	Median	0.025	0.975
J_{96}	number of fry	U(1e5, 1e9)	6.1e+05	5.7e+05	2.8e+05	1.2e+06
J_{97}		U(1e5, 1e9)	2.7e+06	2.6e+06	1.5e+06	4.5e+06
J_{98}		U(1e5, 1e9)	5.3e+06	5.3e+06	3.9e+06	7.1e+06
J_{99}		U(1e5, 1e9)	1.6e+06	1.6e+06	1.1e+06	2.3e+06
γ_0	θ_1 model parameter	N(0, 4)	-2.6e-01	-3.3e-01	-8.0e-01	6.9e-01
γ_1	θ_1 model parameter	N(0, 4)	-7.0e-03	-7.1e-03	-9.7e-03	-5.2e-03
δ_0	j_t model parameter	N(0, 4)	-5.2e+00	-5.2e+00	-6.1e+00	-4.2e+00
δ_1	j_t model parameter	N(0, 4)	8.8e-01	8.7e-01	4.7e-02	1.8e+00
ω	j_t model precision	G(3, 3)	1.3	1.2	6.0e-01	2.2
θ_2	strength of density dependence	U(0, 1)	3.2e-08	2.8e-08	7.8e-09	8.0e-08
CV_J	CV of recruitment stochasticity	see caption	1.4e-01	1.2e-01	2.7e-02	3.7e-01
j_{96}	fry survival probability		3.0e-03	1.8e-03	2.5e-04	1.3e-02
j_{97}			4.7e-03	4.5e-03	2.6e-03	8.0e-03
j_{98}			3.3e-03	3.3e-03	2.4e-03	4.5e-03
j_{99}			1.2e-02	1.2e-02	8.3e-03	1.8e-02
j_{00}			3.8e-03	3.8e-03	2.4e-03	5.4e-03
j_{01}			1.8e-03	1.8e-03	1.2e-03	2.6e-03
j_{02}			4.1e-03	4.0e-03	2.7e-03	5.5e-03
j_{03}			4.1e-03	4.1e-03	3.0e-03	5.5e-03
j_{04}			1.1e-03	1.1e-03	8.3e-04	1.5e-03
j_{05}			6.3e-04	6.2e-04	4.2e-04	8.9e-04
j_{06}			8.0e-04	7.8e-04	5.4e-04	1.2e-03
j_{07}			8.7e-04	8.5e-04	6.5e-04	1.2e-03
j_{08}			1.2e-03	1.2e-03	8.3e-04	1.5e-03
j_{09}			1.2e-03	1.2e-03	7.6e-04	1.6e-03
j_{10}			6.6e-03	6.5e-03	4.7e-03	8.8e-03
j_{11}			4.9e-03	4.9e-03	3.5e-03	6.6e-03
j_{12}			2.6e-03	2.5e-03	1.9e-03	3.5e-03
j_{13}			2.2e-03	1.3e-03	1.8e-04	9.5e-03

Table 6. Mode and median of the forecasted distributions under three forecasting scenarios and the post-hoc $E^0_{t,3}$ values.

	Median			Mode			
Year	*Base*	*ETF*	*no JPI*	*Base*	*ETF*	*JPI*	$E^0_{t,3}$
2012	11559	37950	7682	5803	16948	3718	3294
2013	3482	22825	4222	1676	8846	1711	5971
2014	2537	12381	2866	1128	4549	1523	3063
2015	4420	11856	5091	1814	4097	2356	3742

Table 7. Mean error (ME), root mean square error (RMSE), and log pointwise predictive density (LPPD) for one-year ahead forecasts over 2012–2015. Values of ME and RMSE closer to zero indicate better forecasting performance, whereas higher values of LPPD indicate better performance.

	ME		RMSE		
Scenario	Mode	Median	Mode	Median	LPPD
Base	1129.87	-1185.75	2526.46	2651.42	-9.30
ETF	-3674.07	-13788.20	8215.48	30831.36	-10.32
no JPI	1352.28	-758.32	3023.78	1695.66	-9.47

Table 8. Post-hoc estimates of juvenile survival $\tilde{j}_t$, hatchery-origin juvenile survival $j_{t,o=h}$ estimated from cohort reconstructions, and empirical egg-to-fry survival Z_t for years 2002–2015. Values and direction relative to the median are presented.

	Values			Direction		
Year (t)	$\tilde{j}_t$	$j_{t,o=h}$	Z_t	$\tilde{j}_t$	$j_{t,o=h}$	Z_t
2002	6.01e-03	1.99e-02	0.22	+	+	-
2003		3.39e-03	0.26		-	
2004		2.00e-03	0.21		-	
2005	1.90e-03	2.35e-02	0.30	+	+	+
2006	2.77e-03	1.70e-02	0.24	+	+	+
2007	6.61e-04	9.18e-04	0.22	-	-	-
2008	2.96e-04	1.11e-03	0.23	-	-	-
2009	4.80e-04	3.34e-03	0.18	-	-	-
2010	7.37e-04	3.41e-03	0.23	-	-	-
2011	4.40e-04	2.53e-04	0.19	-	-	-
2012	3.90e-04	7.46e-03	0.40	-	+	+
2013	3.51e-03	4.43e-03	0.46	+	+	+
2014	2.47e-03	5.12e-03	0.55	+	+	+
2015	1.61e-03	6.92e-03	0.48	+	+	+

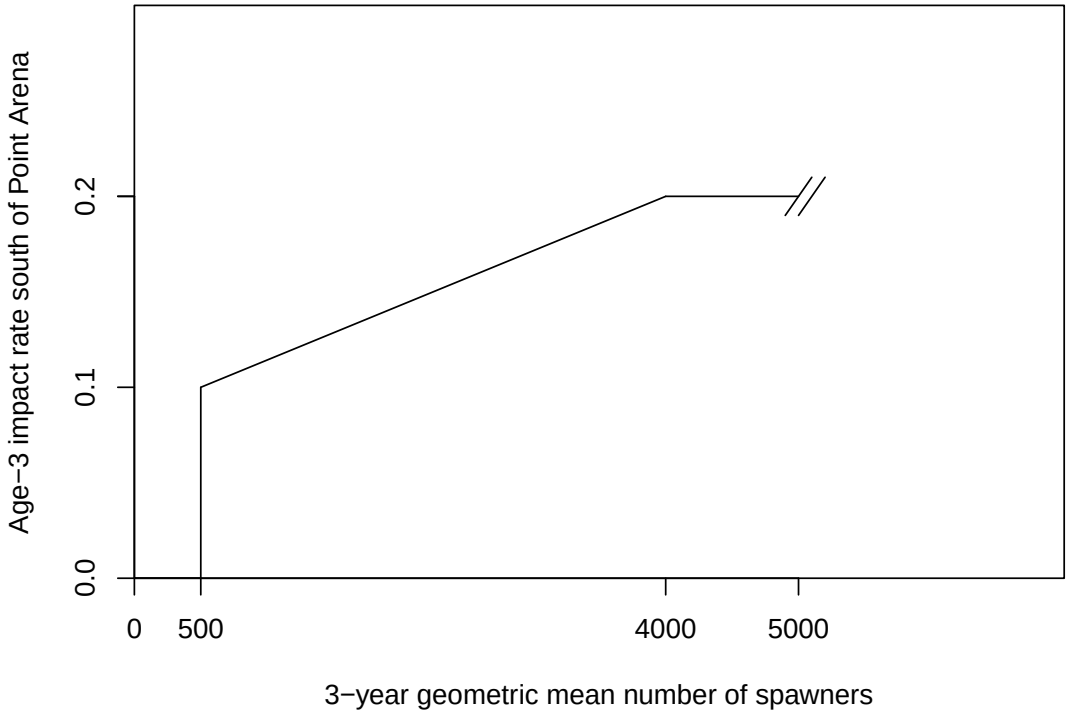

Figure 1. Current Sacramento River winter Chinook fishery control rule.

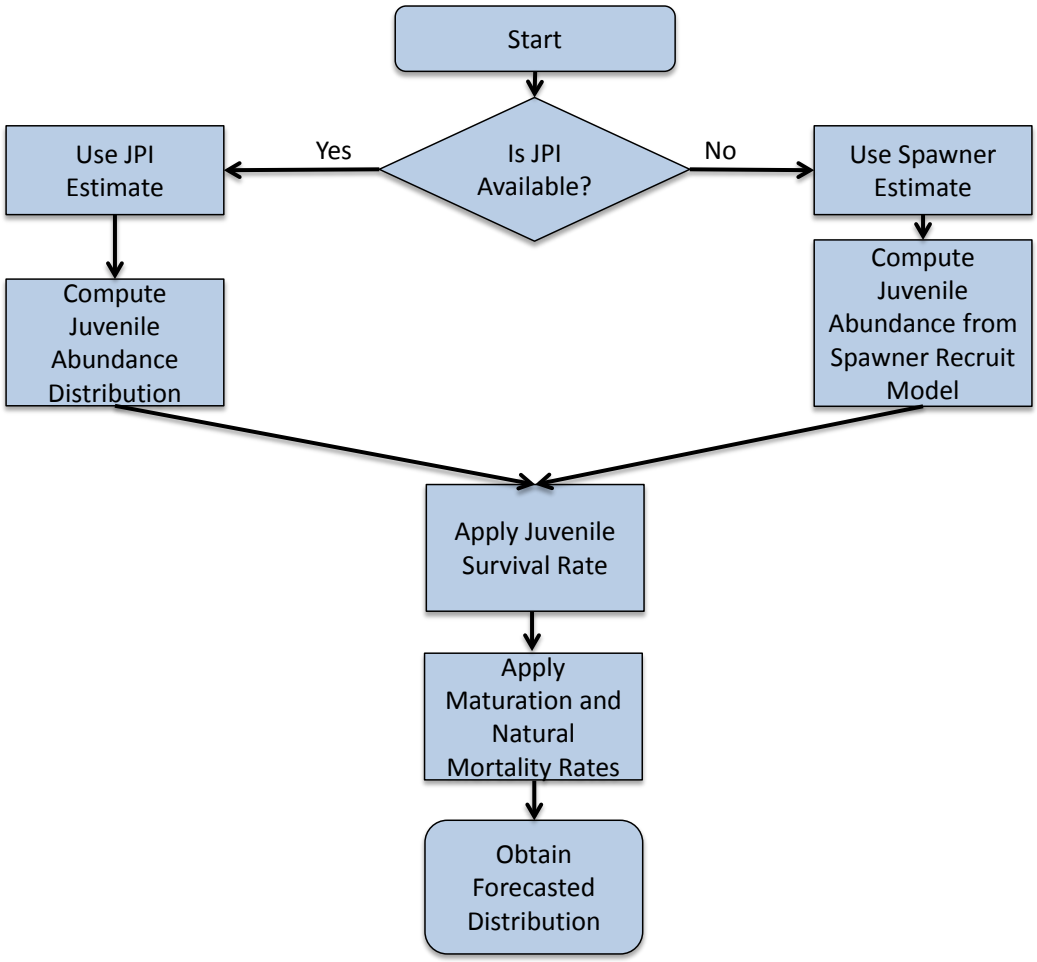

Figure 2. Schematic diagram of natural-origin forecast approaches based on availability of the fry-equivalent Juvenile Production Index (JPI).

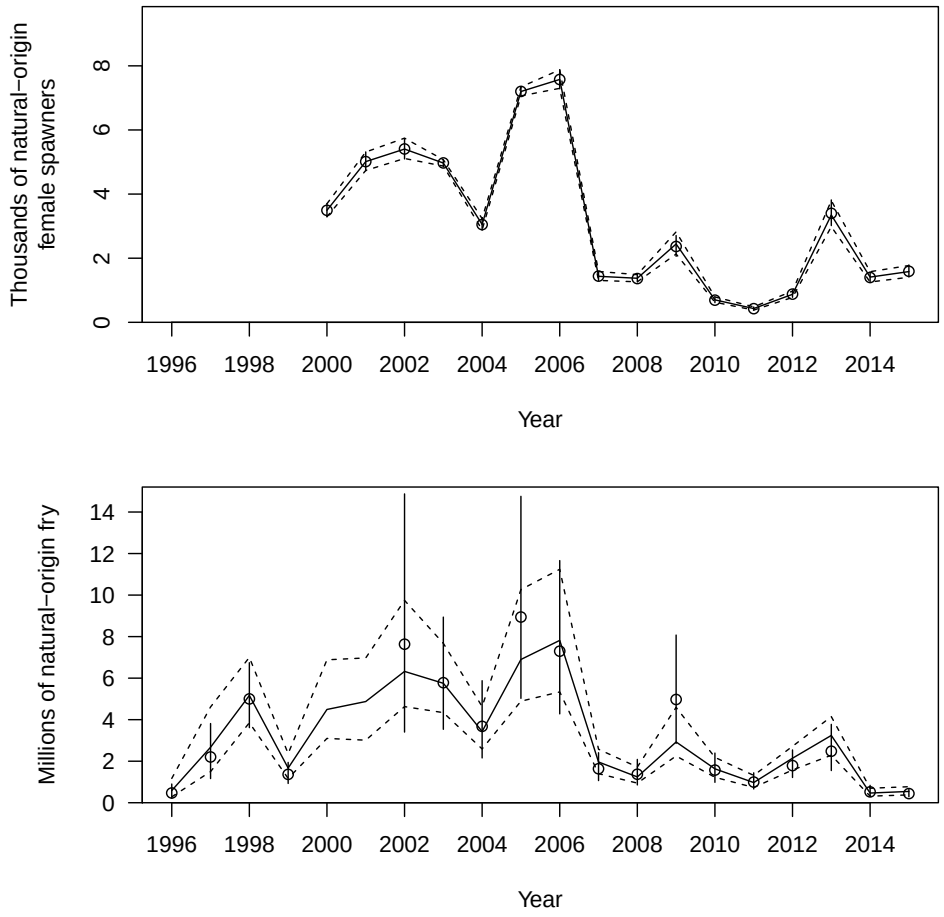

Figure 3. Base model fits to the numbers of natural-origin females spawning in the river and the numbers of natural-origin fry. The circles represent the data and the vertical solid lines represent their assumed 95% confidence intervals. The other solid lines that connect the annual median model estimates and the dashed lines indicate the 95% intervals of posterior probability.

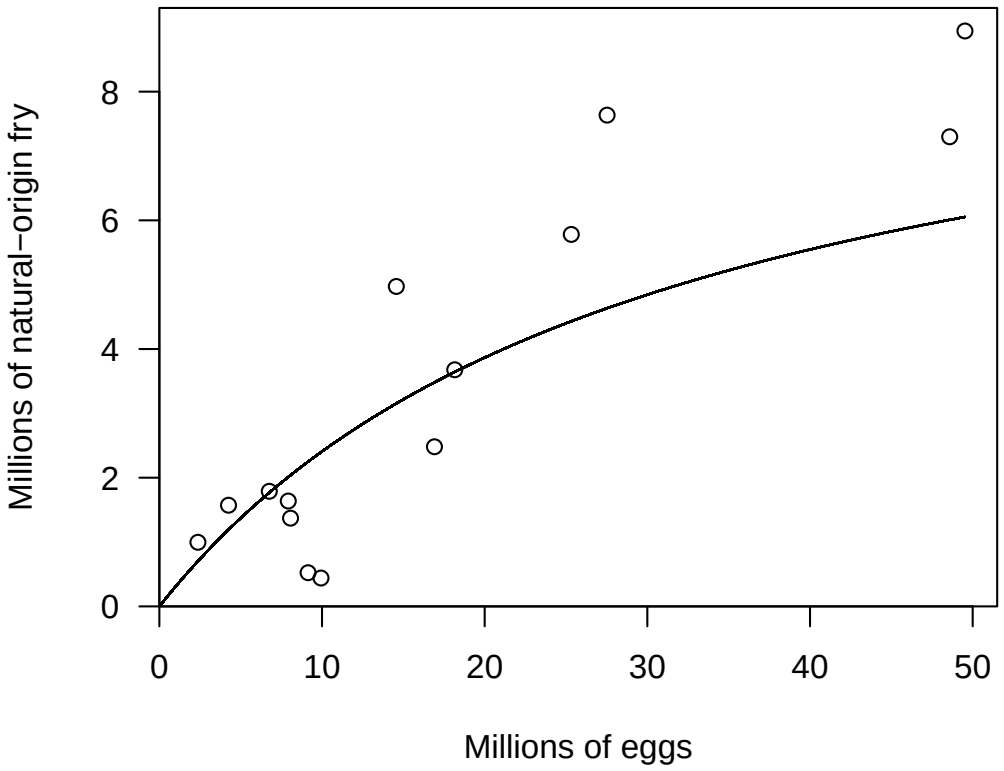

Figure 4. Estimated egg-to-fry relationship evaluated at the mean value of the temperature covariate (X_t).

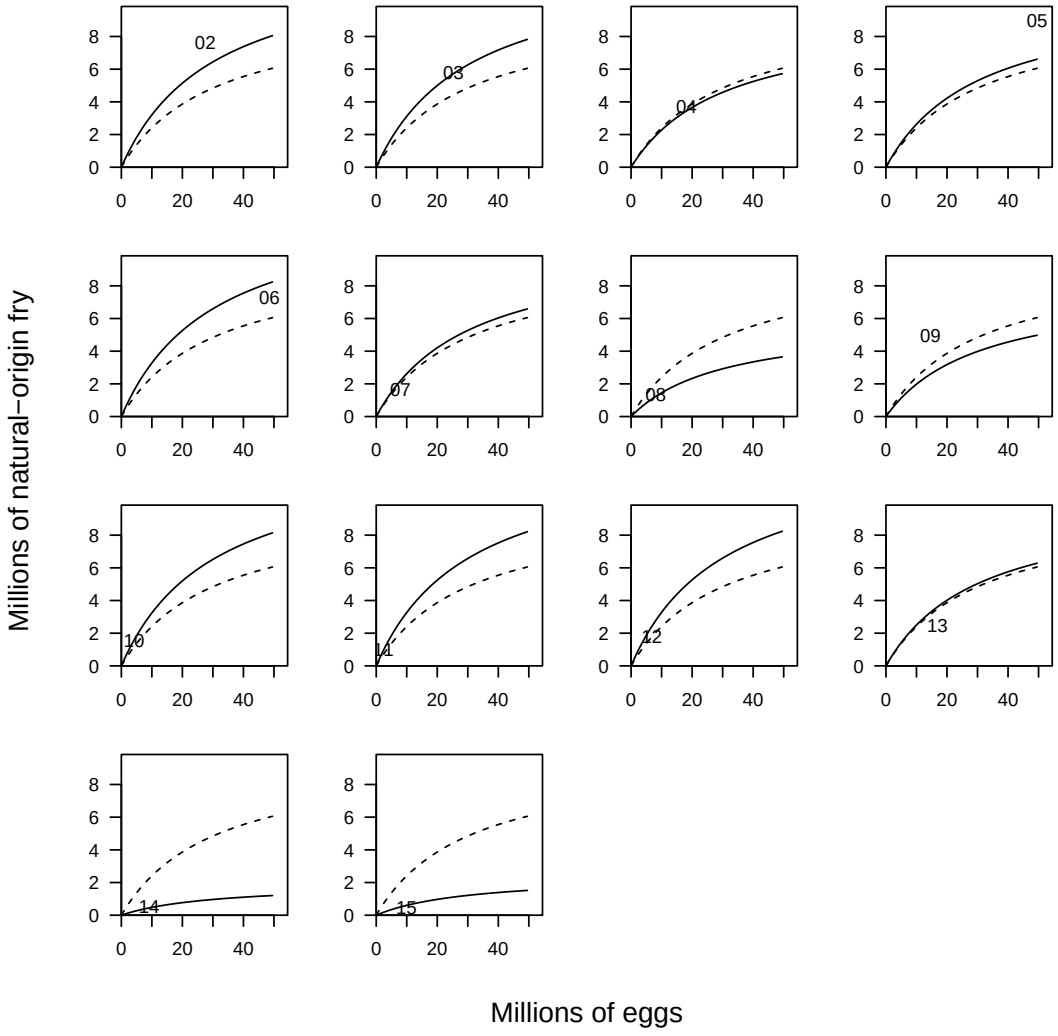

Figure 5. Annual estimated egg-to-fry relationships (solid line) and the estimated egg-to-fry relationship evaluated at the mean value of the temperature covariate (X) (dashed line). Numbers represent brood years.

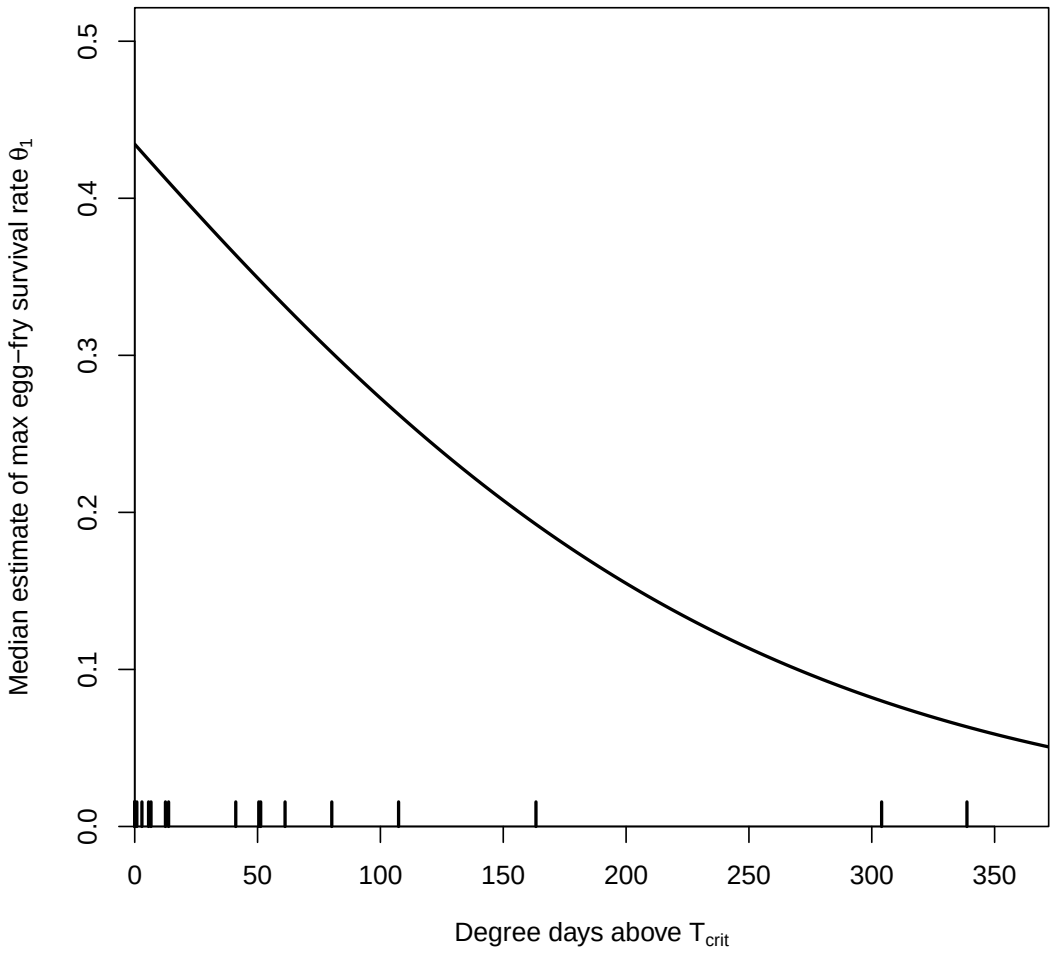

Figure 6. Estimated model (equation 5) of the maximum egg-to-fry survival rate (θ_1) against the temperature covariate (X). Short vertical lines depict actual values of the temperature covariate included in estimation.

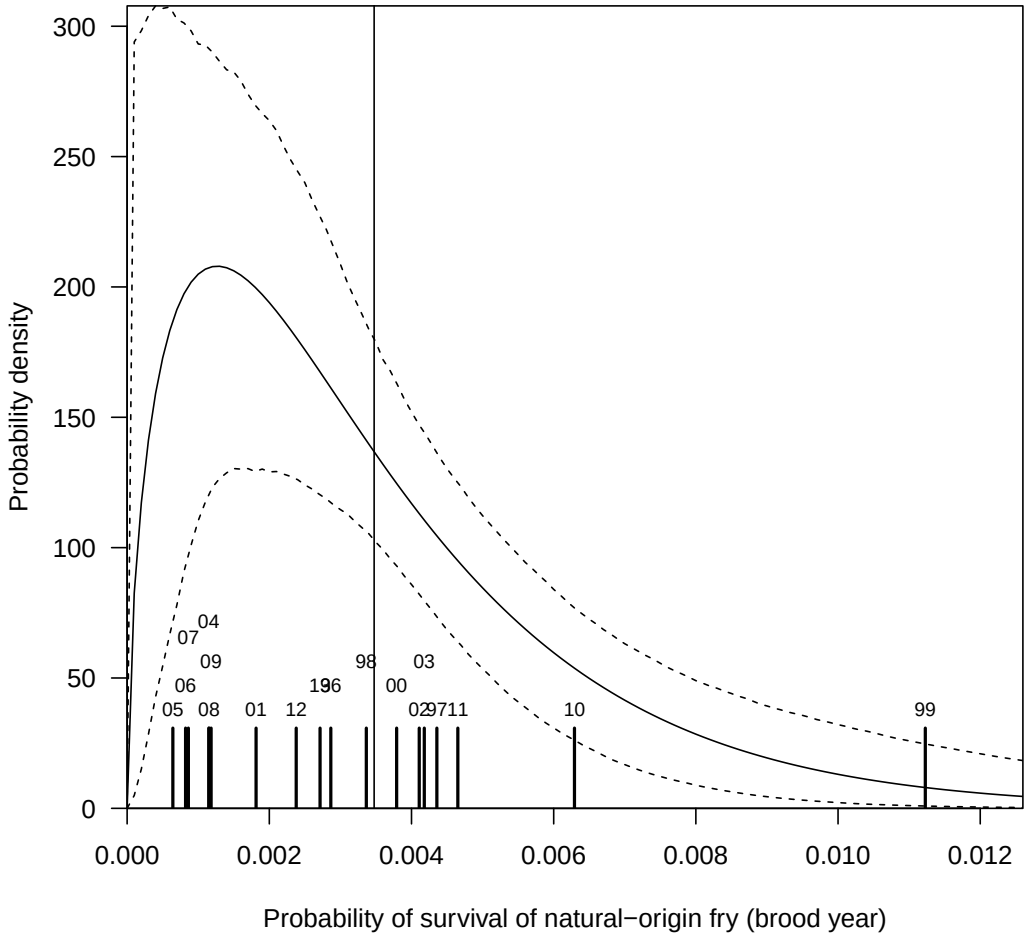

Figure 7. Estimated juvenile survival rate of natural-origin fry. The short vertical bars represent the median estimated survival rates for each brood year. The tall vertical bar represents the posterior median estimate of the mean survival rate. The curved solid line represents the beta distribution fitted to the juvenile survival rates. The dashed lines represent the 95% interval of posterior probability for the distribution of survival probabilities.

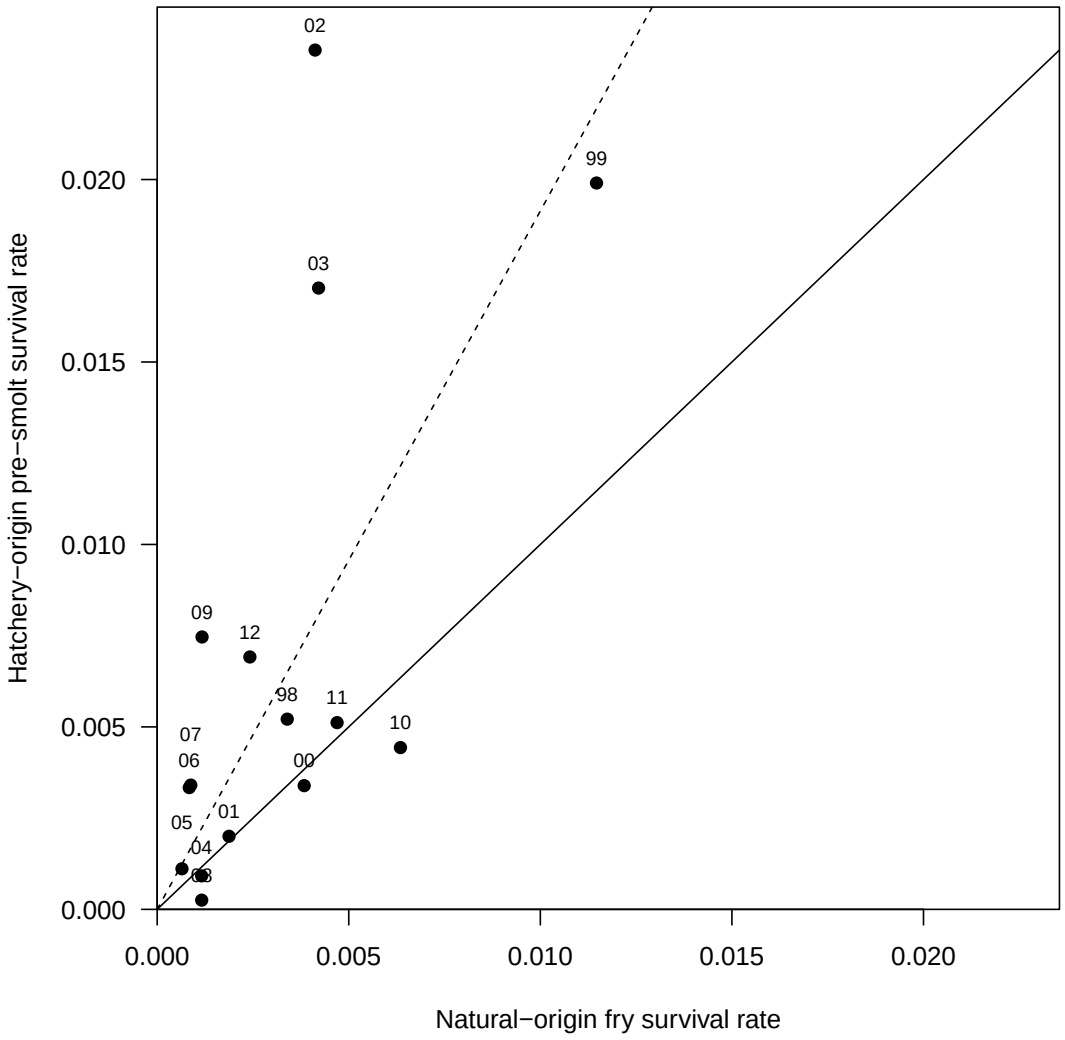

Figure 8. Survival of hatchery-origin juveniles plotted as a function of the natural-origin juvenile survival rate. The 1:1 line is represented by the solid line. The dashed line represents the zero-intercept linear model fitted to these data, with slope estimated using the ratio-of-means estimator.

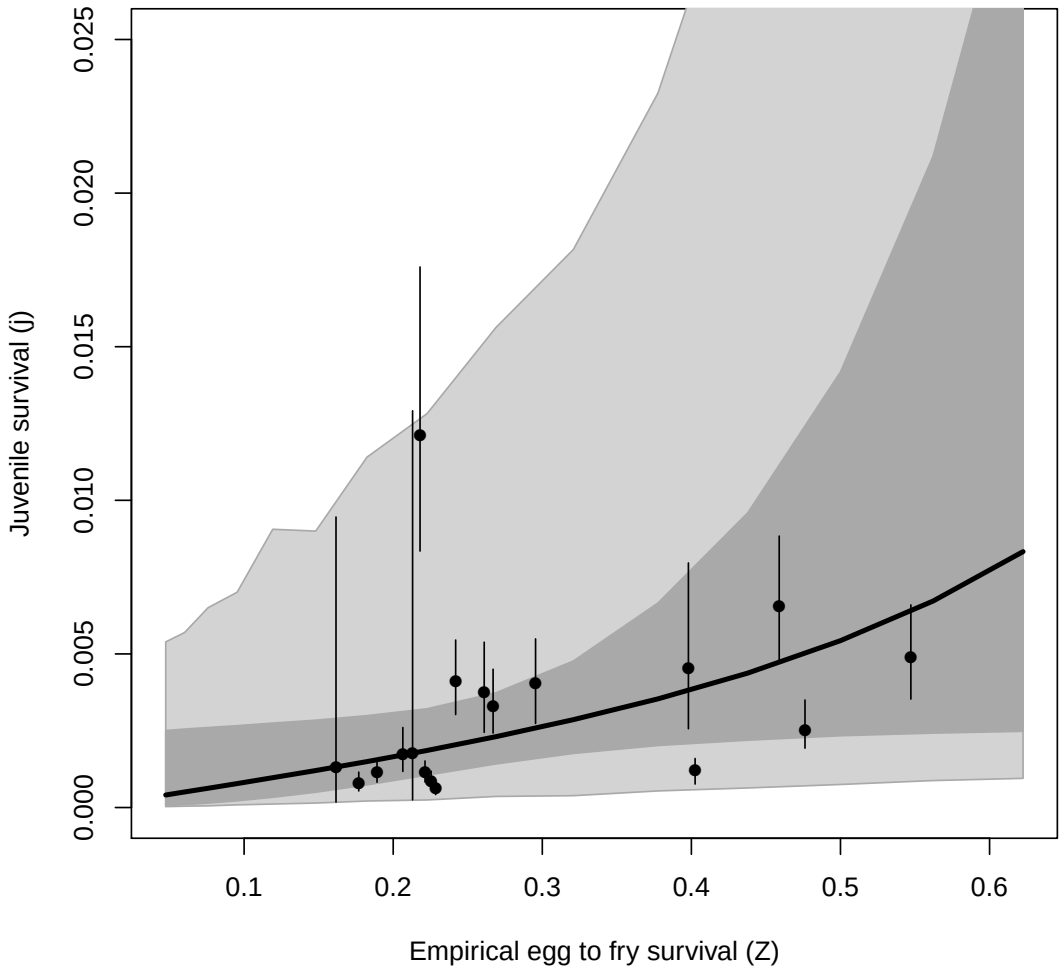

Figure 9. Relationship of juvenile survival rate j to the empirical egg-to-fry survival rate in the *ETF* model. The median relationship is depicted by the dark solid line, the relationship incorporating parameter uncertainty only is depicted by the dark gray region, and the relationship incorporating random effects is depicted by the light gray region. Estimated annual median juvenile survival rates are indicated by the points and the 95% credible intervals are represented by the vertical lines.

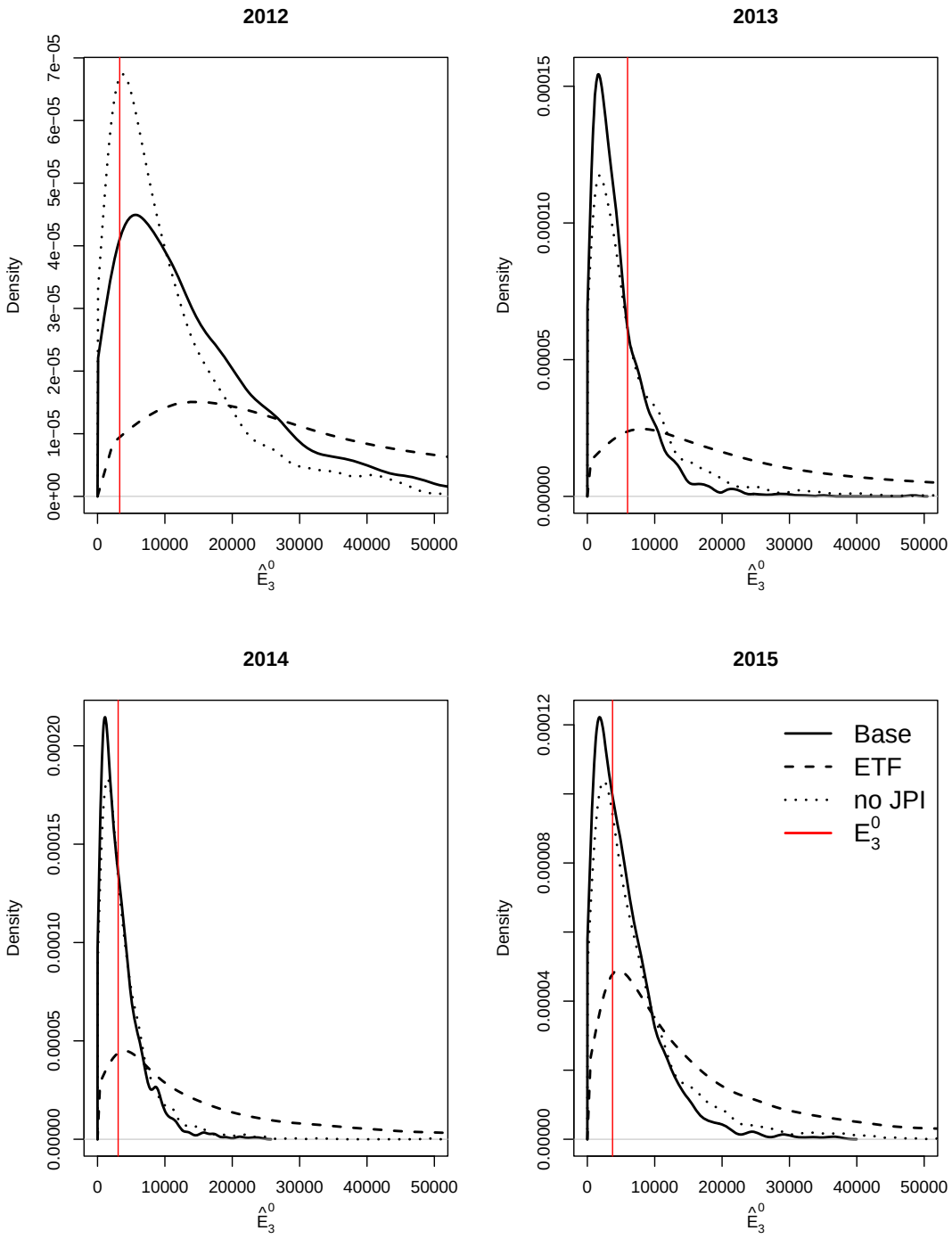

Figure 10. One-year ahead forecasts for escapement in the absence of fishing $\hat{E}^0_{t,3}$ from the *Base*, *ETF*, and *no JPI* models compared to the calculated $E^0_{t,3}$ values.

References

King, R., B. Morgan, O. Gimenez, and S. Brooks (2009). *Bayesian analysis for population ecology*. CRC Press.

Martin, B., A. Pike, S. John, N. Hamda, J. Roberts, and E. Danner (2016). Phenomenological vs. mechanistic models of thermal stress. In review. Ecology Letters.

Mohr, M. S. (2006). The Klamath Ocean Harvest Model (KOHM): parameter estimation. Unpublished report. National Marine Fisheries Service, Santa Cruz, CA.

NMFS (2004). Supplemental Biological Opinion, on authorization of ocean salmon fisheries developed in accordance with the Pacific Coast Salmon Plan and proposed protective measures during the 2004 through 2009 fishing seasons as it affects Sacramento River Winter Chinook salmon. National Marine Fisheries Service, Southwest Region, Protected Resources Division.

NMFS (2010). Authorization of ocean salmon fisheries pursuant to the Pacific Coast Salmon Fishery Management Plan and additional protective measures as it affects Sacramento River Winter Chinook Salmon. National Marine Fisheries Service, Southwest Region, Protected Resources Division.

NMFS (2012). Final implementation of the 2010 Reasonable and Prudent Alternative Sacramento River winter-run Chinook management frameowrk for the Pacific Coast Salmon Fishery Management Plan. Memorandum for: Sacramento River winter Chinook ocean salmon fishery consultation file 151422SWR2009PR00139. From: Fodney R. McInnis, Regional Administrator, NMFS Southwest Region.

O'Farrell, M. R., M. S. Mohr, A. M. Grover, and W. H. Satterthwaite (2012). Sacramento River winter Chinook cohort reconstruction: analysis of ocean fishery impacts. U.S. Dept. Commer., NOAA Tech. Memo. NOAA-TM-NMFS-SWFSC-491, 68p.

PFMC (2016). Review of 2015 ocean salmon fisheries: stock assessment and fishery evaluation

document for the Pacific Coast Salmon Fishery Management Plan. Pacific Fishery Management Council, 7700 NE Ambassador Place, Suite 101, Portland, Oregon 97220-1384.

Plummer, M. (2016). JAGS: A program for analysis of Bayesian graphical models using Gibbs sampling. Version 4.2.0, http://mcmc-jags.sourceforge.net/.

Poytress, W. R. (2016). Brood-year 2014 wintern Chinook Juvenile Production Indices with comparisons to Juvenile Production Estimates derived from adult escapement. U.S. Fish and Wildlife Service, Red Bluff Fish and Wildlife Office, 10950 Tyler Road, Red Bluff, CA, 96080.

Poytress, W. R., J. J. Gruber, F. D. Carrillo, and S. D. Voss (2014). Compendium report of Red Bluff Diversion Dam rotary trap juvenile anadromous fish production indices for years 2002-2012. U.S. Fish and Wildlife Service, Red Bluff Fish and Wildlife Office, 10950 Tyler Road, Red Bluff, CA, 96080.

Winship, A. J., M. R. O'Farrell, and M. S. Mohr (2011). Estimation of paramether for the Sacramento River winter Chinook management strategy evaluation. Report to the Soutwest Region, NMFS.

Winship, A. J., M. R. O'Farrell, and M. S. Mohr (2012). Management Strategy Evaluation for Sacramento River winter Chinook salmon. Report to the Soutwest Region, NMFS.

Winship, A. J., M. R. O'Farrell, and M. S. Mohr (2013). Management strategy evaluation applied to the conservation of an endangered population subject to incidental take. *Biological Conservation 158*, 155–166. http://dx.doi.org/10.1016/j.biocon.2012.08.031.

Winship, A. J., M. R. O'Farrell, and M. S. Mohr (2014). Fishery and hatchery effects on an endangered salmon population with low productivity. *Transasctions of the American Fisheries Society 143*, 957–971. doi: 10.1080/00028487.2014.892532.